JACS
JOURNAL OF THE AMERICAN CHEMICAL SOCIETY
Article
pubs.acs.org/JACS

Examining the Effects of Ligand Variation on the Electronic Structure of Uranium Bis(imido) Species

John J. Kiernicki,[†] Maryline G. Ferrier,[‡] Juan S. Lezama Pacheco,[§] Henry S. La Pierre,[‡] Benjamin W. Stein,[‡] Matthias Zeller,[†,∥] Stosh A. Kozimor,[‡] and Suzanne C. Bart*[,†]

[†]H.C. Brown Laboratory, Department of Chemistry, Purdue University, West Lafayette, Indiana 47907, United States
[‡]Los Alamos National Laboratory, Los Alamos, New Mexico 87545, United States
[§]Stanford University, Stanford, California 94305, United States
[∥]Department of Chemistry, Youngstown State University, Youngstown, Ohio 44555, United States

Supporting Information

ABSTRACT: Arylazide and diazene activation by highly reduced uranium(IV) complexes bearing trianionic redox-active pyridine(diimine) ligands, $[Cp^{P}U(^{Mes}PDI^{Me})]_2$ (**1-Cp^{P}**), Cp*U(^{Mes}PDI^{Me})(THF) (**1-Cp***) (Cp^{P} = 1-(7,7-dimethylbenzyl)cyclopentadienide; Cp* = η^5-1,2,3,4,5-pentamethylcyclopentadienide), and Cp*U(^{t}Bu-^{Mes}PDI^{Me})(THF) (**1-^{t}Bu**) (2,6-((Mes)N=CMe)2-*p*-R-C_5H_2N, Mes = 2,4,6-trimethylphenyl; R = H, ^{Mes}PDI^{Me}; R = $C(CH_3)_3$, ^{t}Bu-^{Mes}PDI^{Me}), has been investigated. While **1-Cp*** and **1-Cp^{P}** readily reduce N_3R (R = Ph, *p*-tolyl) to form *trans*-bis(imido) species, $Cp^{P}U(NAr)_2(^{Mes}PDI^{Me})$ (Ar = Ph, **2-Cp^{P}**; Ar = *p*-Tol, **3-Cp^{P}**) and $Cp^*U(NPh)_2(^{Mes}PDI^{Me})$ (**2-Cp***), only **1-Cp*** can cleave diazene N=N double bonds to form the same product. Complexes **2-Cp***, **2-Cp^{P}**, and **3-Cp^{P}** are uranium(V) *trans*-bis(imido) species supported by neutral $[^{Mes}PDI^{Me}]^0$ ligands formed by complete oxidation of $[^{Mes}PDI^{Me}]^{3-}$ ligands of **1-Cp^{P}** and **1-Cp***. Variation of the arylimido substituent in **2-Cp*** from phenyl to *p*-tolyl, forming $Cp^*U(NTol)_2(^{Mes}PDI^{Me})$ (**3-Cp***), changes the electronic structure, generating a uranium(VI) ion with a monoanionic pyridine(diimine) radical. The *tert*-butyl-substituted analogue, Cp*U(NTol)$_2$(^{t}Bu-^{Mes}PDI^{Me}) (**3-^{t}Bu**), displays the same electronic structure. Oxidation of the ligand radical in **3-Cp*** and **3-^{t}Bu** by Ag(I) forms cationic uranium(VI) $[Cp^*U(NTol)_2(^{Mes}PDI^{Me})][SbF_6]$ (**4-Cp***) and $[Cp^*U(NTol)_2(^{t}Bu\text{-}^{Mes}PDI^{Me})][SbF_6]$ (**4-^{t}Bu**), respectively, as confirmed by metrical parameters. Conversely, oxidation of pentavalent **2-Cp*** with $AgSbF_6$ affords cationic $[Cp^*U(NPh)_2(^{Mes}PDI^{Me})][SbF_6]$ (**5-Cp***) from a metal-based U(V)/U(VI) oxidation. All complexes have been characterized by multidimensional NMR spectroscopy with assignments confirmed by electronic absorption spectroscopy. The effective nuclear charge at uranium has been probed using X-ray absorption spectroscopy, while structural parameters of **1-Cp^{P}**, **3-Cp***, **3-^{t}Bu**, **4-Cp***, **4-^{t}Bu**, and **5-Cp*** have been elucidated by X-ray crystallography.

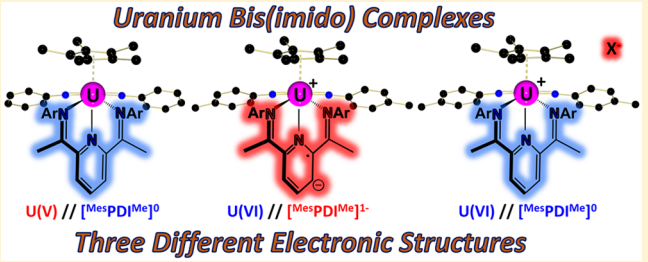

INTRODUCTION

Redox noninnocent ligands have grown in popularity in recent years due to their ability to mediate reactions that would otherwise not be possible.[1,2] Their unique chemical properties and reactivity are useful in synthetic applications;[3−6] however, understanding the exact role of these ligands in such transformations can be difficult due to their redox flexibility, often generating derivatives whose electronic structures are difficult to characterize.[7−11] One of the best studied examples is that of the pyridine(diimine) ligand, which rose to fame due to its ability to support highly active ethylene polymerization catalysts.[12,13] Since this time, this ligand system has been established to exist in a variety of oxidation states and electronic structures, depending on whether it is chelated to a p-block,[14,15] d-block,[3,16] or f-block metal.[17−19]

The popularity of such a ligand stems from its ability to mediate multielectron transfer reactions, which have broad applications in many areas, including small molecule activation, catalysis, and bioinorganic chemistry. Pairing this framework with an electron-rich metal like uranium results in highly reducing dimers that perform 8- and 12-electron transfers.[17] Introducing further variation with additional ancillary ligands offers steric blocking and tunability at these large metal centers. In 2013, our laboratory reported the synthesis of Cp*U(^{Mes}PDI^{Me})(THF) (**1-Cp***), which is a uranium(IV) species bearing a triply reduced pyridine(diimine) chelate, $[^{Mes}PDI^{Me}]^{3-}$.[19] This electron-rich uranium compound effectively cleaves the N=N double bond of azobenzene, resulting in the formation of the uranium(V) *trans*-bis(imido), Cp*U(^{Mes}PDI^{Me})(NPh)$_2$ (**2-Cp***).[19] This four-electron reduction is accomplished using one electron from uranium and all three

Received: July 6, 2016
Published: October 12, 2016

DOI: 10.1021/jacs.6b06989
J. Am. Chem. Soc. 2016, 138, 13941−13951

reducing equivalents from $[^{Mes}PDI^{Me}]^{3-}$, leaving an overall neutral $^{Mes}PDI^{Me}$ chelate, $[^{Mes}PDI^{Me}]^{0}$. Treating **1-Cp*** with an oxygen transfer reagent generates the uranyl analogue, $Cp^*UO_2(^{Mes}PDI^{Me})$, formed from another four-electron transfer. In this case, spectroscopic and structural analyses support a uranium(VI) ion ligated by a pyridine(diimine) ligand radical, $[^{Mes}PDI^{Me}]^{1-}$, supporting that two electron oxidation events occurred at both the ligand and the metal.

Given the drastic change in ground-state electronic structure that results with only small changes of uranium substituents, we sought to explore the effect of ligand substitution further. Changing the substitution of the cyclopentadienyl ring, from five methyl groups to a single dimethylbenzyl group, leads to the **1-Cp*** analogue, $[Cp^PU(^{Mes}PDI^{Me})]_2$ (**1-Cp^P**).[20] On the basis of the superior electron-donating ability of **1-Cp***, we hypothesized there would be a difference in reactivity of **1-Cp^P** toward diazenes as compared to **1-Cp*** due to the poorly electron-donating character of the Cp^P ligand. Herein, we present our studies examining the differences in reactivity of **1-Cp*** and **1-Cp^P** toward strong oxidants such as PhN═NPh, TolN═NTol, N_3Ph, and N_3Tol, with the effects of imido substituent and pyridine(diimine) ligand substitution also examined. Our findings suggest that subtle differences in electron-donating capability associated with the cyclopentadienyl rings impart marked changes in reactivity, facilitating the synthesis of a family of uranium bis(imido) products that can exist in three different electronic structure classifications. Identification of products and electronic structure assignments are aided by spectroscopic and structural analysis.

EXPERIMENTAL SECTION

All air- and moisture-sensitive manipulations were performed using standard Schlenk techniques or in an MBraun inert atmosphere drybox with an atmosphere of purified nitrogen. The MBraun drybox was equipped with a cold well designed for freezing samples in liquid nitrogen as well as two −35 °C freezers for cooling samples and crystallizations. Solvents for sensitive manipulations were dried and deoxygenated using literature procedures with a Seca solvent purification system.[21] Benzene-d_6 and chloroform-d were purchased from Cambridge Isotope Laboratories, dried with molecular sieves and sodium (C_6D_6) or CaH_2 ($CDCl_3$), and degassed by three freeze−pump−thaw cycles. Celite was dried by heating to 120 °C under vacuum overnight. Azobenzene (Sigma-Aldrich) and silver hexafluoroantimonate (Alfa Aesar) were purchased and used as received. Arylazides,[22] 1,2-bis(4-methylphenyl)-diazene (Tol−N═N−Tol),[23] $Cp^*U(^{Mes}PDI^{Me})(THF)$ (**1-Cp***),[19] $Cp^*U(^tBu\text{-}^{Mes}PDI^{Me})(THF)$ (**1-^{t}Bu**),[24] $[Cp^PU(^{Mes}PDI^{Me})]_2$ (**1-Cp^P**),[20] and $AgBPh_4$[25] were prepared according to literature procedures.

^{1}H NMR spectra were recorded on a Varian Inova 300 spectrometer operating at 299.992 MHz. All chemical shifts are reported relative to the peak for $SiMe_4$, using ^{1}H (residual) chemical shifts of the solvent as a secondary standard. The spectra for paramagnetic molecules were obtained by using an acquisition time of 0.5 s; thus the peak widths reported have an error of ±2 Hz. For paramagnetic molecules, the ^{1}H NMR data are reported with the chemical shift, followed by the peak width at half height in hertz, the integration value, and, where possible, the peak assignment. Elemental analyses were performed by Complete Analysis Laboratories, Inc., Parsippany, NJ. Electronic absorption spectroscopic measurements were recorded at 294 K in sealed 1 cm quartz cuvettes with a Cary 6000i UV−vis−NIR spectrophotometer. Infrared spectra were recorded using either a PerkinElmer FT-IR Spectrum RX I or a Nicolet 6700 FT-IR spectrometer. Samples were prepared on KBr salt plates. A full description of X-ray absorption spectroscopic experimental details is provided in the Supporting Information.

Single crystals of **3-Cp*** suitable for X-ray diffraction were coated with poly(isobutylene) oil in a glovebox and quickly transferred to the goniometer head of a Nonius KappaCCD image plate diffractometer equipped with a graphite crystal, incident beam monochromator. Preliminary examination and data collection were performed with Mo Kα radiation (λ = 0.71073 Å). In a similar fashion, single crystals of **1-Cp^P**, **3-^{t}Bu**, and **4-^{t}Bu** suitable for X-ray diffraction were transferred to the goniometer head of a Rigaku Rapid II image plate diffractometer equipped with a MicroMax002+ high intensity copper X-ray source with confocal optics. Preliminary examination and data collection were performed with Cu Kα radiation (λ = 1.54184 Å). Single crystals of **4-Cp*** and **5-Cp*** were transferred to a Bruker AXS D8 Quest CMOS diffractometer equipped with a complementary metal−oxide−semiconductor (CMOS) detector and an I-μ-S Mo Kα microsource X-ray tube (λ = 0.71073 Å) operated at 50 kV and 1 mA with laterally graded multilayer (Goebel) mirror X-ray optics. Structures were solved with SHELXS[26] and refined using the graphical user interface ShelXle[27] for the refinement program SHELXL.[28]

The U $L_{3,2}$-edge X-ray measurements were carried out on uranium samples that had been triply contained. Samples were prepared under a nitrogen atmosphere. The samples were diluted with boron nitride (BN), which was dried at elevated temperature (200 °C) under vacuum (10^{-3} Torr) for 24 h prior to use. A mixture of the analyte and BN was weighed out, such that the edge jump for the absorbing atom was calculated to be at 1 absorption length in transmission (~30−50 mg of sample and 50−30 mg of BN). Samples were ground using a Wiggle Bug using a Teflon bead and a polycarbontate capsule. The finely ground powders were pressed as a pellet into a slotted aluminum sample holder equipped with a Kapton windows (1.0 mm); one was fixed with super glue and the other was with Kapton tape. This primary holder was nested within a secondary aluminum holder equipped with Kapton (2.0 mm) windows that were sealed with indium wire. The samples were sealed in ziplock bags, placed in sealed polypropylene jars, and shipped to SSRL. Once unpackaged, the samples were immediately attached to the coldfinger of a liquid N_2 cryostat and quickly evacuated (10^{-7} Torr). The cryostat was attached to the beamline 11-2 XAFS rail (SSRL), which was equipped with three ionization chambers through which nitrogen gas was continually flowed. One chamber (10 cm) was positioned before the cryostat to monitor the incident radiation (I_0). The second chamber (30 cm) was positioned after the cryostat so that sample transmission (I_1) could be evaluated against I_0 and so that the absorption coefficient (μ) could be calculated as $\ln(I_0/I_1)$. The third chamber (I_2; 30 cm) was positioned downstream from I_1 so that the XANES of a calibration foil could be measured against I_1. A potential of 1600 V was applied in series to the ionization chambers. Samples were calibrated in situ to the energy of the first inflection point of the K-edge of an yttrium foil (17 038.4 eV).

The X-ray absorption near edge spectra (XANES) were measured at the Stanford Synchrotron Radiation Lightsource (SSRL) under dedicated operating conditions (3.0 GeV, 5%, 500 mA using continuous topoff injections) on end station 11-2. This beamline, which was equipped with a 26-pole, 2.0 T wiggler, utilized a liquid nitrogen-cooled double-crystal Si[220] monochromator and employed collimating and focusing mirrors. A single energy was selected from the white beam with a liquid-N_2-cooled double-crystal monochromator utilizing Si[220] (φ = 0) crystals. Harmonic rejection was achieved by detuning the second crystal of the monochromator by 35% at 17 766 eV. The horizontal and vertical slit sizes were 10 and 1 mm, respectively.

Synthesis of $Cp^PU(NPh)_2(^{Mes}PDI^{Me})$ (2-Cp^P). A 20 mL scintillation vial was charged with 0.109 g (0.133 mmol) of $[Cp^PU(^{Mes}PDI^{Me})]_2$ and 4 mL of toluene. While being stirred, 0.032 g (0.269 mmol) of phenylazide was added, resulting in the liberation of N_2(g). After 15 min, volatiles were removed in vacuo. The resulting solid was washed with cold *n*-pentane (−35 °C) to afford a dark brown solid (0.109 g, 0.109 mmol, 82%) assigned as $Cp^PU(NPh)_2(^{Mes}PDI^{Me})$. Anal. Calcd for $C_{53}H_{56}N_5U$: C, 63.59; H, 5.64; N, 7.00. Found: C, 63.49; H, 5.79; N, 6.92. ^{1}H NMR (C_6D_6, 25 °C): δ = −16.63 (74, 2H, Ar−C*H*), −12.44 (80, 1H, Ar−C*H*), −11.70 (108, 4H, Ar−C*H*), −7.03 (3, 2H, Ar−C*H*), −5.21 (52, 6H, CH_3), −4.15

DOI: 10.1021/jacs.6b06989
J. Am. Chem. Soc. 2016, 138, 13941−13951

(62, 6H, CH_3), −3.28 (55, 2H, Ar−C*H*), −1.58 (22, 2H, Ar−C*H*), 0.01 (94, 4H, Ar−C*H*), 3.99 (22, 2H, Ar−C*H*), 4.46 (16, 2H, Ar−C*H*), 11.32 (48, 4H, Ar−C*H*), 22.24 (163, 12H, o−Ar−CH_3), 28.25 (28, 6H, CH_3), 30.73 (4, 1H, Ar−C*H*).

Alternate Synthesis of Cp*U(NPh)$_2$(^{Mes}PDI^{Me}) (2-Cp*). A 20 mL scintillation vial was charged with 0.100 g (0.118 mmol) of **1-Cp*** and 4 mL of toluene. While being stirred, 0.029 g (0.243 mmol) of phenylazide was added, resulting in liberation of N_2(g). After 5 min, volatiles were removed in vacuo. The resulting solid was washed with cold *n*-pentane (−35 °C) to afford a dark brown solid (0.067 g, 0.070 mmol, 59%) confirmed as Cp*U(NPh)$_2$(^{Mes}PDI^{Me}) by ^{1}H NMR spectroscopic analysis.

Synthesis of Cp^{P}U(NTol)$_2$(^{Mes}PDI^{Me}) (3-Cp^P). Prepared analogously to **2-Cp^P** with *p*-tolN$_3$ (dark brown powder; yield, 82%). Anal. Calcd for $C_{55}H_{60}N_5U$: C, 64.19; H, 5.88; N, 6.80. Found: C, 63.88; H, 5.87; N, 6.49. ^{1}H NMR (C_6D_6, 25 °C): δ = −11.56 (100, 12H, *o*-Ar−CH_3), −5.37 (76, 4H, Ar−C*H*), −4.10 (32, 6H, CH_3), −0.06 (260, 4H, Ar−C*H*), 0.43 (80, 2H, Ar−C*H*), 4.07 (129, 4H, Ar−C*H*), 4.56 (77, 2H, Ar−C*H*), 6.30 (855, 2H, Ar−C*H*), 7.40 (558, 2H, Ar−C*H*), 14.67 (200, 2H, Ar−C*H*), 14.98 (84, 6H, CH_3), 17.16 (16, 1H, Ar−C*H*), 22.08 (61, 1H, Ar−C*H*), 23.25 (159, 6H, CH_3), 29.31 (975, 6H, CH_3).

Synthesis of Cp*U(NTol)$_2$(^{Mes}PDI^{Me}) (3-Cp*). A 20 mL scintillation vial was charged with **1-Cp*** (0.225 g, 0.266 mmol) and 10 mL of toluene. While being stirred, Tol−N=N−Tol (0.056 g, 0.266 mmol) was added. After being stirred for 15 min, volatiles were removed in vacuo. The resulting solid was recrystallized from a saturated pentane solution at −35 °C to afford a dark brown solid (0.212 g, 0.216 mmol, 81%) assigned as Cp*U(NTol)$_2$(^{Mes}PDI^{Me}). Single, X-ray quality crystals were grown from a concentrated toluene/*n*-pentane (1:10) solution at −35 °C. Anal. Calcd for $C_{51}H_{60}N_5U$: C, 62.44; H, 6.16; N, 7.14. Found: C, 62.27; H, 6.34; N, 7.03. ^{1}H NMR (C_6D_6, 300 MHz, 25 °C): δ = 1.39 (s, 3H, N=CCH_3), 1.64 (s, 3H, N=CCH_3), 1.99 (s, 6H, Ar−CH_3), 2.04 (s, 6H, Ar−CH_3), 2.22 (s, 6H, Ar−CH_3), 3.12 (s, 6H, Tol−CH_3), 4.15 (d, *J* = 5, 1H, *m*-pyr−C*H*), 4.51 (s, 15H, Cp*), 5.54 (m, 1H, *p*-pyr−C*H*), 5.96 (d, *J* = 8, 4H, Tol−C*H*), 6.70 (d, *J* = 16, 1H, pyr−C*H*), 6.81 (s, 2H, *m*-Ar−C*H*), 6.82 (s, 2H, *m*-Ar−C*H*), 7.45 (d, *J* = 8, 4H, Tol−C*H*). ^{13}C NMR (C_6D_6, 126 MHz, 25 °C): δ = 8.69 (Cp*−CH_3), 18.21 (N=CCH_3), 18.56 (*p*tol−CH_3), 19.37 (N=CCH_3), 19.65 (Mes−CH_3), 20.80 (Mes−CH_3), 21.44 (Mes−CH_3), 30.18 (*m*-pyr−C*H*), 111.51 (*p*-pyr−C*H*), 124.20 (*p*tol−C*H*), 124.65 (*m*-pyr−C*H*), 125.70, 129.34, 129.52, 132.84, 133.79, 134.60, 135.02, 135.94, 136.37, 140.14 (*p*tol−C*H*), 146.07 (C=N−*C*), 155.30, 166.54 (N=*C*CH_3), 171.25 (N=*C*CH_3).

Synthesis of Cp*U(NTol)$_2$(^{t}Bu-^{Mes}PDI^{Me}) (3-^{t}Bu). Prepared analogously to **3-Cp*** with Tol−N=N−Tol (brown powder; yield, 56%). Single, X-ray quality crystals were obtained from a concentrated *n*-pentane solution at −35 °C. Anal. Calcd for $C_{59}H_{68}N_5U$: C, 63.69; H, 6.61; N, 6.75. Found: C, 63.67; H, 6.63; N, 6.95. ^{1}H NMR (C_6D_6, 500 MHz, 25 °C): δ = 1.35 (s, 9H, ^{t}Bu−CH_3), 1.70 (s, 3H, N=CCH_3), 1.75 (s, 3H, N=CCH_3), 2.00 (s, 6H, CH_3), 2.04 (s, 6H, CH_3), 2.22 (s, 6H, CH_3), 3.12 (s, 6H, *p*-tol−CH_3), 4.18 (s, 1H, *m*-pyr−C*H*), 4.50 (s, 15H, Cp*), 5.89 (d, *J* = 8.0, 4H, *o*-tol−C*H*), 6.65 (s, 1H, *m*-pyr−C*H*), 6.83 (s, 2H, *m*-Ar−C*H*), 6.83 (s, 2H, *m*−Ar−C*H*), 7.43 (d, *J* = 8.0, 4H, *m*-tol−C*H*). ^{13}C NMR (C_6D_6, 25 °C): δ = 8.73 (Cp*−CH_3), 18.19 (*p*tol−CH_3), 18.31 (N=CCH_3), 18.58 (CH_3), 19.37 (N=CCH_3), 19.64 (CH_3), 20.83 (CH_3), 28.83 (C(CH_3)$_3$), 29.83 (*m*-pyr−CH), 35.35 (*C*(CH_3)$_3$), 116.16 (*m*-pyr−CH), 124.14 (*p*tol−CH), 125.33, 125.70, 129.51 (Ar−CH), 129.53 (Ar−CH), 133.07, 133.54, 134.63, 134.89, 135.82, 136.34, 140.12 (*p*tol−CH), 146.42, 155.27, 167.85 (N=*C*CH_3), 170.44 (N=*C*CH_3).

Synthesis of [Cp*U(NTol)$_2$(^{Mes}PDI^{Me})][SbF$_6$] (4-Cp*). A 20 mL scintillation vial was charged with Cp*U(NTol)$_2$(^{Mes}PDI^{Me}) (0.114 g, 0.116 mmol) and 5 mL of THF. While being stirred, $AgSbF_6$ was added, and the mixture was stirred for 2 h. The solution was filtered over Celite, and volatiles were removed in vacuo. The resulting solid was washed with *n*-pentane until the washings were clear and dried to yield a brown powder (0.095 g, 0.078 mmol, 67%) assigned as [Cp*U(NTol)$_2$(^{Mes}PDI^{Me})][SbF_6]. Single, X-ray quality crystals precipitated from a concentrated THF/diethyl ether (3:1) solution stored at room temperature. Anal Calcd for $C_{51}H_{60}N_5SbF_6U$: C, 50.34; H, 4.97; N, 5.76. Found: C, 50.10; H, 5.18; N, 6.26. ^{1}H NMR (C_6D_6, 300 MHz, 25 °C): δ = 1.63 (s, 12H, *o*-Ar−CH_3), 2.02 (s, 6H, CH_3), 2.13 (s, 6H, CH_3), 3.20 (s, 6H, *p*-tol−CH_3), 4.96 (s, 15H, Cp*), 5.02 (d, *J* = 8, 4H, *p*-tol−C*H*), 6.64 (s, 4H, *m*-Ar−C*H*), 7.49 (d, *J* = 8, 4H, *p*-tol−C*H*), 8.91 (d, *J* = 8, 2H, *m*-pyr−C*H*), 9.22 (t, *J* = 8, 1H, *p*-pyr−C*H*). ^{13}C NMR ($CDCl_3$, 126 MHz, 25 °C): δ = 7.81 (Cp*−CH_3), 18.11 (*p*tol−CH_3), 18.83 (*o*-Mes−CH_3), 19.77 (CH_3), 20.63 (CH_3), 124.01 (*p*tol−CH), 130.13 (*m*-Mes−CH), 130.63, 132.33 (*m*-pyr−CH), 137.17, 139.16 (*p*tol−CH), 139.52, 139.92, 143.40, 144.07 (*p*tol−CH), 155.06 (*C*−N=(Me) (Pyr)), 157.48 (N=C−C_{pyr}), 177.67 (N=*C*CH_3).

Synthesis of [Cp*U(NTol)$_2$(^{t}Bu-^{Mes}PDI^{Me})][SbF$_6$] (4-^{t}Bu). Prepared analogously to **4-Cp*** from **3-^{t}Bu** (brown powder; yield, 94%). Single, X-ray quality crystals of the analogous tetraphenylborate complex precipitated from a concentrated THF/hexamethyldisiloxane (3:1) solution stored at room temperature. Anal. Calcd for $C_{79}H_{88}N_5B_1U$: C, 69.95; H, 6.54; N, 5.16. Found: C, 70.42; H, 6.32; N, 4.86. ^{1}H NMR (C_6D_6, 300 MHz, 25 °C): δ = 1.75 (s, 12H, *o*-Ar−CH_3), 2.04 (s, 9H, C(CH_3)$_3$, 2.23 (s, 6H, CH_3), 2.45 (s, 6H, CH_3), 3.26 (s, 6H, *p*tol−CH_3), 5.05 (s, 15H, Cp*), 5.08 (d, *J* = 7.8, 4H, *o*-tol−C*H*), 6.73 (s, 4H, *m*-Ar−C*H*), 7.49 (d, *J* = 7.8, 4H, *m*-tol−C*H*), 8.98 (s, 2H, *m*-pyr−C*H*). ^{13}C NMR ($CDCl_3$, 25 °C): δ 7.50 (Cp*−CH_3), 18.16 (*p*tol−CH_3), 18.65 (*o*-Mes−CH_3), 20.19 (CH_3), 20.75 (CH_3), 30.43 (C(CH_3)$_3$), 36.68 (*C*(CH_3)$_3$), 123.50 (*o*-tol−CH), 129.37 (*m*-pyr−CH), 130.18 (Mes−CH), 137.58, 138.73 (*m*-tol−CH), 138.88, 140.25, 142.85, 155.66 (*C*−N=(Me) (Pyr)), 157.03 (N=C−C_{pyr}), 168.43 (*p*-pyr−CH), 176.78 (N=*C*CH_3).

Synthesis of [Cp*U(NPh)$_2$(^{Mes}PDI^{Me})][SbF$_6$] (5-Cp*). Prepared analogously to **4-Cp*** from **2-Cp*** (red-brown powder; yield, 89%). Single, X-ray quality crystals were obtained by slow diffusion of *n*-pentane into a concentrated THF solution of **5-Cp***. Anal. Calcd for $C_{49}H_{56}N_5SbF_6U$: C, 49.51; H, 4.75; N, 5.89. Found: C, 49.04; H, 4.79; N, 5.38. ^{1}H NMR (C_6D_6, 300 MHz, 25 °C): δ = 1.60 (s, 12H, *o*-Ar−CH_3), 1.98 (s, 6H, CH_3), 2.13 (s, 6H, CH_3), 5.08 (s, 15H, Cp*), 5.08 (4H, *o*-Ph−CH), 5.08 (2H, *p*-Ph−CH) 6.63 (s, 4H, *m*-Ar−CH), 7.70 (t, *J* = 8.1, 4H, *m*-Ph−CH), 8.85 (d, *J* = 8.1, 2H, *m*-pyr−CH), 9.19 (t, *J* = 8.1, 1H, *p*-pyr−CH). ^{13}C NMR (C_6D_6, 25 °C): δ = 7.49 (Cp*−CH_3), 18.77 (*o*-Mes−CH_3), 19.79 (CH_3), 20.68 (CH_3), 124.32 (*m*-Ph−CH), 129.21, 130.17 (Mes−CH), 130.63, 132.39 (*m*-pyr−CH), 137.29, 139.53 (*o*-Ph−CH), 140.59 (*p*-Ph−CH), 143.34, 144.09 (*p*-pyr−CH), 154.94 (*C*−N=(Me) (Pyr)), 158.79 (N=C−C_{pyr}), 177.79 (N=*C*CH_3).

RESULTS AND DISCUSSION

Synthesis of Bis(imido) Complexes. On the basis of our previous findings describing successful azobenzene activation by **1-Cp***, initial studies focused on further characterization of **1-Cp^P** so that direct comparison of Cp ligands could be made and analogous reactivity evaluated. Although the synthesis and spectroscopic characterization of **1-Cp^P** was previously reported[20] and predicted to be the monomeric base-free analogue of **1-Cp***, its molecular structure remained elusive due to the inability to grow suitable crystals for X-ray diffraction analysis. After repeated attempts, single, X-ray quality crystals of **1-Cp^P** precipitated after 4 days from a concentrated THF/*n*-pentane (2:1) solution at −35 °C. Surprisingly, refinement of the data revealed a 1:1 cocrystallized mixture of [Cp^{P}U(^{Mes}PDI^{Me})]$_2$ (**1-Cp^P**) and previously identified [(^{Mes}PDI^{Me})U(THF)]$_2$,[17] each of which contains an inversion center (full structure and parameters presented in Figures S43, S44, and Table S1). Analysis of the mother liquor by ^{1}H NMR spectroscopy revealed various isomers of dimeric 1-(7,7-dimethylbenzyl)cyclopentadiene, suggesting **1-Cp^P** gradually decomposes via homolytic cleavage of Cp^P to form the thermodynamically favorable [(^{Mes}PDI^{Me})U(THF)]$_2$ in the presence of THF.[17]

DOI: 10.1021/jacs.6b06989
J. Am. Chem. Soc. 2016, 138, 13941−13951

In the molecular structure of **1-Cp^P**, each uranium is bound by a pyridine(diimine) as well as an η^5-Cp^P ligand (Figure 1).

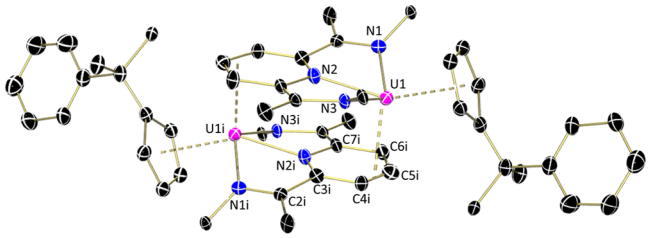

Figure 1. Molecular structure of **1-Cp^P** displayed with 30% probability ellipsoids. 2,4,6-Trimethylphenyl substituents, hydrogen atoms, cocrystallized THF, and [(^{Mes}PDI^{Me})U(THF)]$_2$ have been omitted for clarity.

The uranium−centroid distance (2.540 Å) is similar to those observed in the uranium(IV) analogues Cp^{P}U(X)$_2$(^{Mes}PDI^{Me}) (X = I,[8] Cl, SPh, SePh;[29] U−Ct range: 2.500−2.542 Å), while the U−N distances are nearly identical to isoelectronic [(^{Mes}PDI^{Me})UI]$_2$,[17] confirming a trianionic chelate. Similar to both [(^{Mes}PDI^{Me})UI]$_2$ and [(^{Mes}PDI^{Me})U(THF)]$_2$, the uranium centers in **1-Cp^P** are bonded to the pyridine ring of the opposing half, 0.851 Å above the plane of the three chelating nitrogen atoms. Here, this interaction is best described as η^3 (U1−Ct$_{(C4i-C5i-C6i)}$ = 2.694 Å), rather than the η^5 interaction noted for [(^{Mes}PDI^{Me})UI]$_2$ and [(^{Mes}PDI^{Me})U(THF)]$_2$. This decreased hapticity of the pyridine ring is also reflected by an increased U1−U1i distance (6.971 Å) as compared to [(^{Mes}PDI^{Me})UI]$_2$ and [(^{Mes}PDI^{Me})U(THF)]$_2$ (3.741 and 3.668 Å, respectively).[18] Vapor pressure lowering experiments suggest the dimerization of **1-Cp^P** is maintained in solution. This is consistent with the calculated energies of dimerization for structurally similar [(^{Mes}PDI^{Me})UI]$_2$ and [(^{Mes}PDI^{Me})U(THF)]$_2$ of −116.0 and −144.4 kcal/mol, respectively. It is likely that the dimeric nature of **1-Cp^P** should not preclude reactivity toward diazenes as [(^{Mes}PDI^{Me})UI]$_2$ was previously shown to effectively reduce both Mes−N=N−Mes and N$_3$Mes.[17]

With the molecular structure of **1-Cp^P** confirmed, its reactivity was tested by adding 1 equiv of PhN=NPh. No reaction occurred, even after heating the mixture, which caused decomposition of **1-Cp^P** with no evidence for azobenzene consumption or formation of the desired uranium(V) bis(imido) compound, Cp^{P}U(NPh)$_2$(^{Mes}PDI^{Me}) (**2-Cp^P**). Addition of 2 equiv of the more reactive phenylazide, N$_3$Ph, furnished **2-Cp^P**, as evident from N$_2$(g) evolution and darkening of the solution (Scheme 1). Confirmation of brown **2-Cp^P** was obtained by ^{1}H NMR spectroscopy (Figure S1), which showed a paramagnetically broadened and shifted C_{2v} symmetric spectrum with 15 resonances (−17 to 30 ppm), similar to Cp*U(NPh)$_2$(^{Mes}PDI^{Me}) (**2-Cp***).[19] The analogous phenylazide activation can also be performed to generate **2-Cp*** from **1-Cp***.

Isolation of **2-Cp^P** indicates that steric hindrance does not prevent diazene activation; instead, the inability of **1-Cp^P** to activate diazenes is likely due its diminished reducing ability in comparison to **1-Cp***, which is expected given that the dimethylbenzyl substituent is much less electron-donating than the five methyl groups of Cp*. Overall, generation of **2-Cp^P** and **2-Cp*** occurs from a four-electron transfer, with three electrons obtained from oxidation of [^{Mes}PDI^{Me}]$^{3-}$ to neutral [^{Mes}PDI^{Me}]^0 and one electron derived from oxidation from U(IV) to U(V).

While multielectron activation of 2 equiv of organoazide is the favored route for **1-Cp^P**, using only 1 equiv of N$_3$Ph does not produce the corresponding uranium mono(imido), Cp^{P}U(NPh)(^{Mes}PDI^{Me}), but instead results in 0.5 equiv of **2-Cp^P** and 0.5 equiv of unreacted **1-Cp^P**, suggesting a facile second two-electron redox process.

The effect of the variation of the diazene or azide substituent on the resulting bis(imido) electronic structure was probed. 1,2-Bis(4-methylphenyl)-diazene (Tol−N=N−Tol) was an attractive choice due to its structural similarity but more negative reduction potential as compared to azobenzene (−1.604 and −1.746 V, vs Fc/Fc$^+$, Figure S30). Not surprisingly, **1-Cp^P** was unreactive toward Tol−N=N−Tol, with no observation of the corresponding bis(imido) complex; however, 2 equiv of *para*-tolylazide (*p*-TolN$_3$) cleanly generated Cp^{P}U(NTol)$_2$(^{Mes}PDI^{Me}) (**3-Cp^P**) (Scheme 1),

Scheme 1. Synthesis of Bis(imido) Complexes 2 and 3 Bearing the Cp^P and Cp* Ligands via Arylazide and Diazene Reductions

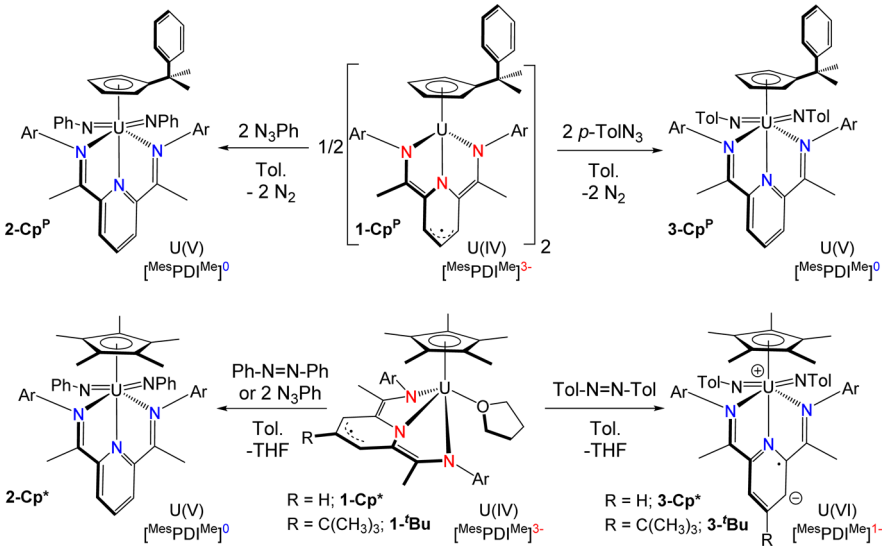

DOI: 10.1021/jacs.6b06989
J. Am. Chem. Soc. 2016, 138, 13941−13951

which has a ^{1}H NMR spectrum analogous to that of **2-Cp^P** (Figure S2).

To confirm that **2-Cp***, **2-Cp^P**, and **3-Cp^P** are isoelectronic, electronic absorption spectroscopy was employed (Figure 3, top; Figures S36–S38). Data were collected from 280 to 1800 nm in THF at ambient temperature. All complexes display broad, featureless spectra throughout the visible regions as well as a pair of weakly intense, sharp absorbances in the near-infrared regions indicative of uranium(V) ions. For **2-Cp***, these absorptions appear at 1615 (ε = 388.34 M^{-1} cm^{-1}) and 1657 nm (ε = 106.27 M^{-1} cm^{-1}), while for **2-Cp^P** and **3-Cp^P** the energies of these absorptions are slightly blue-shifted. For **2-Cp^P** and **3-Cp^P**, the higher energy absorbance is hypochromically shifted as compared to **2-Cp***, consistent with decreasing electron donation of Cp^P as compared to Cp*. Similar f–f transitions and trends in extinction coefficients have been noted for the uranium(V) mono(imido), Cp*$_2$U(NDIPP)(X),[30] mono(oxo), N*$_3$UO(X) (N* = N(SiMe$_3$)$_2$), and bis(halide), N*$_3$UX$_2$ (X = halide, pseudohalide, alkyl, or aryl) species.[31] By charge balance considerations, **2-Cp^P** and **3-Cp^P** contain neutral pyridine(diimine) ligands, as in **2-Cp***. It should be noted that the increased electron donicity from the *para*-methyl in **3-Cp^P** does not influence the overall electronic structure, maintaining the 5f^1 ground state.

In contrast to **1-Cp^P**, treating a toluene solution of **1-Cp*** with 1 equiv of Tol–N=N–Tol resulted in an immediate reaction as indicated by darkening of the solution (Scheme 1). Following workup, analysis of the brown powder by ^{1}H NMR spectroscopy revealed 14 sharp resonances ranging from 1.39 to 7.45 ppm consistent with a C_s symmetric product in solution and formation of Cp*U(NTol)$_2$(^{Mes}PDI^{Me}) (**3-Cp***) (Figure 2). The observed sharpness and peak distribution for **3-Cp*** diverge from the broad, ill-defined resonances observed for **2-Cp***, **2-Cp^P**, and **3-Cp^P**, suggesting a different electronic structure, and is reminiscent of that observed for Cp*UI(^{Mes}PDI^{Me}), featuring a closed-shell pyridine(diimine) dianion, which ranges from −2.21 to 7.96 ppm (25 °C, C$_6$D$_6$).[20]

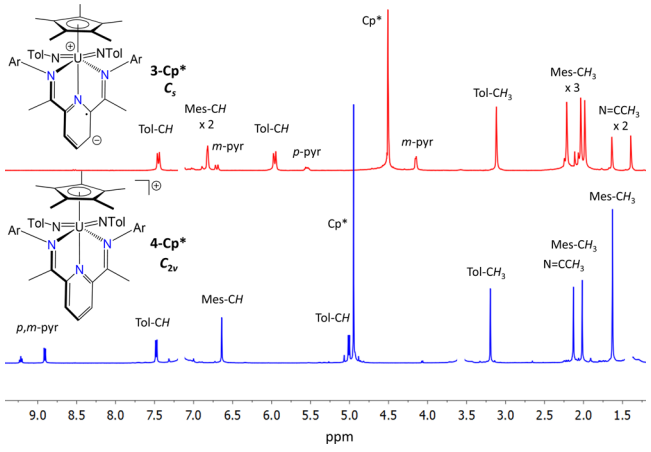

Figure 2. ^{1}H NMR spectra (C$_6$D$_6$, 25 °C) of **3-Cp*** (top) and **4-Cp*** (bottom) reported in ppm. Residual solvent resonances have been omitted to improve clarity. Unabridged spectra are presented in Figure S29.

Consistent with the C_s assignment for **3-Cp***, there is an intense singlet assignable to the pentamethylcyclopentadienyl protons (15H, 4.51 ppm), while three resonances (6H each) are assigned to the aryl–C*H*$_3$ protons (Figure 2, top). A pair of resonances integrating to three protons each results from inequivalent imine methyl protons in the plane of the pyridine. Aryl(imido) resonances are observed at 3.12 (C*H*$_3$), 5.96 (d, J = 8), and 7.45 (d, J = 8) ppm. Two pairs of doublets (4.15, 6.70 ppm) and a multiplet (5.54 ppm) confirm asymmetry in the pyridine(diimine) chelate.

The chemical shift of these pyridine resonances warranted further investigation by 2D NMR spectroscopy. An HMQC spectrum revealed that the pyridine–C*H* resonances (confirmed by DEPT-135 experiments, Figure S7) of 4.15 (*m*), 5.54 (*p*), and 6.70 (*m*) ppm correspond to respective ^{13}C chemical shifts of 30.18, 111.51, and 124.65 ppm (Figure S5). These values suggest an increase in sp^3 character on only one of the *m*-carbons (^{13}C = 30.18 ppm) due to significant charge buildup. This localized electron density is evident from the ^{1}H–^{1}H coupling constants as well. Because the doublets for the C$_{meta}$–H (J = 16, 5) protons are inconsistent with *ortho*-coupling, the C$_{meta}$–C$_{para}$–C$_{meta}$ linkage is best described as allylic, C$_{meta}$H=C$_{para}$H–C$_{meta}$H, with localized electron density on a single carbon. The NMR spectroscopic data of **3-Cp*** are reminiscent of those observed for both Cp*UO$_2$(^{Mes}PDI^{Me}) and Cp*UO$_2$(^{t}Bu-^{Mes}PDI^{Me}), each of which has been fully characterized and is best described as a uranium(VI) uranyl species bearing a singly reduced pyridine(diimine) ligand.[24]

The formation of **3-Cp*** proceeds by a four-electron transfer, with two reducing equivalents derived each from the uranium(IV) center and from [^{Mes}PDI^{Me}]$^{3-}$ of **1-Cp***, leaving a U(VI) ion and [^{Mes}PDI^{Me}]$^{1-}$, as with Cp*UO$_2$(^{Mes}PDI^{Me}). This contrasts with the formation of the uranium(V) analogues, **2-Cp*** and **2-Cp^P**, where the [^{Mes}PDI^{Me}]$^{3-}$ electron reservoir is depleted. The [^{Mes}PDI^{Me}]$^{1-}$ in **3-Cp*** is enforced by the electron-donating *p*-methyl substituents, whereas unsubstituted phenyls lack the electron-donating ability required to stabilize such a reduced ligand.

To confirm ^{Mes}PDI^{Me} reduction in **3-Cp***, X-ray diffraction studies were performed on suitable crystals of this material obtained from a concentrated toluene/*n*-pentane solution (1:10, −35 °C). Refinement of the data revealed a pyridine(diimine) uranium complex with 2-fold symmetry bearing *trans*(imido) ligands (N4–U1–N4′ = 155.9(3)°) capped by an η^5-Cp* (U–Ct = 2.583 Å) in a distorted octahedral environment (Figure 4, left, Table 1). The U–N$_{imido}$ distances (U–N4 = 1.950(7) Å) in **3-Cp*** are significantly longer than those in hexavalent CpU(N^{t}Bu)$_2$I(dmpe) (dmpe = 1,2-bis(dimethylphosphino)ethane) (1.883(4) and 1.889(5) Å), reported by Boncella and co-workers.[32] However, these distances are shorter than those in pentavalent **2-Cp*** (2.036(5), 1.994(6) Å), as would be expected for the smaller U(VI) ion. Although the pyridine(diimine) ligand displays long U–N bonds (U1–N1 = 2.522(6); U1–N2 = 2.515(7) Å), suggestive of dative bonds, inspection of the intraligand distances supports ligand reduction. Such distortions are well established as indicative of population of ligand antibonding orbitals and can be diagnostic of the amount of pyridine(diimine) reduction.[16] This is evident in the C3–C4 bond distance of the pyridine ring, which has been significantly elongated (1.439(10) Å) beyond that expected for an aromatic pyridine (free ligand = 1.386(3), 1.388(3) Å).[17] Such distortions have been observed in tetravalent Cp*U(O$_2$C$_2$Ph$_2$H$_2$)(^{Mes}PDI^{Me}) and hexavalent Cp*UO$_2$(^{Mes}PDI^{Me}), both of which bear [^{Mes}PDI^{Me}]$^{1-}$ ligands as charge separated resonance forms. Contraction of the adjacent C$_{imine}$–C$_{pyridine}$ bond to 1.431(10) Å from that in the free ligand (1.495(3),

DOI: 10.1021/jacs.6b06989
J. Am. Chem. Soc. 2016, 138, 13941–13951

Table 1. Structural Parameters for 3-Cp*, 3-^{t}Bu, 4-Cp*, 4-^{t}Bu, and 5-Cp*[a]

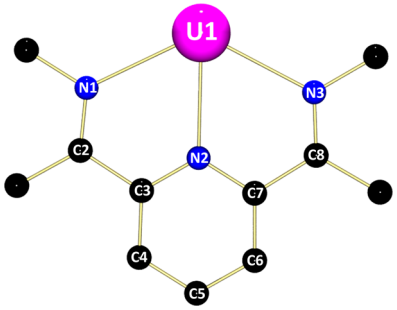

bond (Å) or angle (deg)	3-Cp*	3-^{t}Bu	4-Cp*	4-^{t}Bu	5-Cp*
U1−N1	2.522(6)	2.518(7)	2.549(4)	2.567(4)	2.567(4)
U1−N2	2.515(7)	2.515(7)	2.539(4)	2.508(4)	2.538(4)
U1−N3	2.522(6)	2.524(8)	2.597(4)	2.567(4)	2.580(4)
U1−N4	1.950(7)	1.941(8)	1.928(4)	1.955(4)	1.930(4)
U1−N5	1.950(7)	1.944(8)	1.926(4)	1.944(4)	1.943(4)
N1−C2	1.304(9)	1.316(11)	1.301(6)	1.292(6)	1.291(7)
C2−C3	1.431(10)	1.427(14)	1.484(6)	1.484(6)	1.488(7)
C3−C4	1.439(10)	1.466(14)	1.391(7)	1.410(6)	1.404(7)
C4−C5	1.386(10)	1.368(16)	1.376(7)	1.392(7)	1.369(8)
C5−C6	1.386(10)	1.425(16)	1.387(7)	1.394(7)	1.386(8)
C6−C7	1.439(10)	1.496(13)	1.387(7)	1.404(6)	1.392(7)
N2−C3	1.359(7)	1.347(12)	1.347(6)	1.352(6)	1.340(6)
N2−C7	1.359(7)	1.320(12)	1.346(6)	1.351(6)	1.356(6)
C7−C8	1.431(10)	1.433(14)	1.481(6)	1.486(7)	1.484(7)
N3−C8	1.304(9)	1.327(11)	1.291(7)	1.290(6)	1.290(7)
U1−Ct	2.583	2.567	2.565	2.503	2.531
N4−U1−N5	155.9(3)	155.5(3)	155.45(16)	153.14(15)	154.57(18)

[a]Pyridine(diimine) numbering scheme listed above.

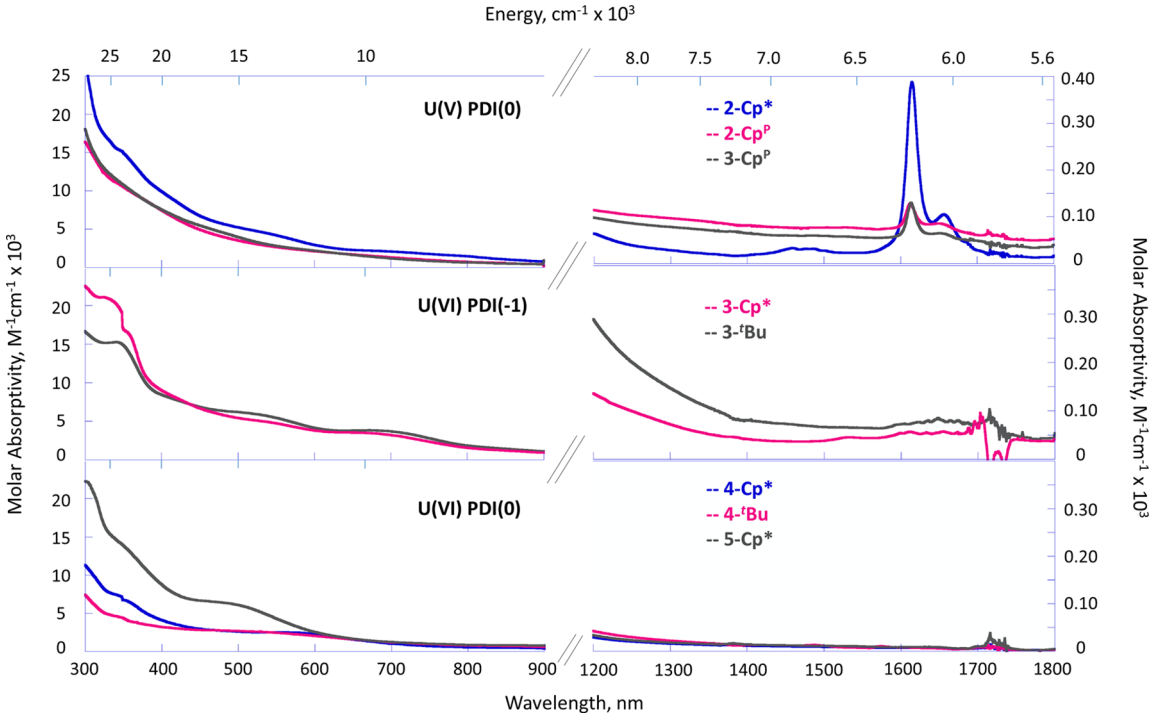

Figure 3. Electronic absorption data collected from 280 to 1800 nm in THF at ambient temperature (solvent overtones are present from 1670 to 1760 nm). Top: Uranium(V)-[^{Mes}PDI^{Me}]^0 complexes **2-Cp***, **2-Cp^P**, and **3-Cp^P**. Middle: Uranium(VI)-[^{Mes}PDI^{Me}]$^{1-}$ complexes **3-^{t}Bu** and **3-Cp***. Bottom: Uranium(VI)-[^{Mes}PDI^{Me}]^0 complexes **4-Cp***, **4-^{t}Bu**, and **5-Cp***.

DOI: 10.1021/jacs.6b06989
J. Am. Chem. Soc. 2016, 138, 13941−13951

1.494(3) Å) also points toward a singly reduced pyridine(diimine) ligand, consistent with the NMR spectroscopic studies.

The unusual ligand electronic structure assignment is corroborated by the electronic absorption spectrum of **3-Cp*** (Figure 3, middle), which is markedly different from those of its uranium(V) counterparts. **3-Cp*** displays a pair of strong absorptions at 672 (3825 M^{-1} cm^{-1}) and 497 nm (6210 M^{-1} cm^{-1}) in the visible region as well as an absorbance in the UV region at 342 nm (15 250 M^{-1} cm^{-1}), all of which are hypothesized to arise from radical character predominantly on the pyridine(diimine) ligand. Further, the broad f−f transitions present in the near-infrared region of **2-Cp*** are not detected in **3-Cp***, suggesting the absence of f-electrons and a U(VI), $5f^0$ ground state.

With significant electronic differences arising from slight alterations of the cyclopentadienyl and aryl(imido) ligands noted, variation to the pyridine(diimine) chelate was also explored by substitution of the hydrogen atom in the *p*-pyridine position with a *tert*-butyl group. Employing Cp*U(^{t}Bu-^{Mes}PDI^{Me})(THF) (**1-^{t}Bu**) as a precursor, attempts to form bis(imido) species analogous to **3-Cp^P** and **3-Cp*** were undertaken. Unfortunately, due to their highly reactive nature, **1-Cp^P**, **1-Cp***, and **1-^{t}Bu** are not amenable to standard electrochemical conditions with each being reactive toward various electrolytes and common solvents (CH_3CN, CH_2Cl_2). However, as [^{t}Bu-^{Mes}PDI^{Me}] is more difficult to reduce than the parent ligand by 0.124 V,[24] we hypothesized three potential outcomes for the reduction of Tol−N═N−Tol by **1-^{t}Bu**: (1) formation of a uranium(VI) bis(imido) species with stabilization of a ligand radical at the *para*-pyridine position by the new tertiary carbon,[33] (2) a uranium(VI) bis(imido) with localized anionic charge at a *meta*-pyridine position similar to **3-Cp***, or (3) isolation of a uranium(V) bis(imido) neutral ligand species analogous to **2-Cp***, **2-Cp^P**, and **3-Cp^P** due to the more negative reduction potential of [^{t}Bu-^{Mes}PDI^{Me}].

Addition of 1 equiv of Tol−N═N−Tol to **1-^{t}Bu** resulted in an immediate darkening of the solution, proof of a successful synthesis of Cp*U(NTol)$_2$(^{t}Bu-^{Mes}PDI^{Me}) (**3-^{t}Bu**) (Scheme 1). Investigation of **3-^{t}Bu** by electronic absorption spectroscopy showed strong transitions, comparable to **3-Cp***, in the visible region at 663 (3503 M^{-1} cm^{-1}) and 530 nm (5834 M^{-1} cm^{-1}), and in the UV region at 324 nm (21 091 M^{-1} cm^{-1}), suggesting the presence of a ligand radical (Figure 3, middle). Coupled with a lack of f−f transitions in the near-infrared region, these spectroscopic data support **3-^{t}Bu** as a uranium(VI) complex with a [^{Mes}PDI^{Me}]$^{1-}$ ligand, eliminating option (3). This formulation is further confirmed by 2D NMR spectroscopy, which shows the peak distribution of C_s symmetric **3-^{t}Bu** to be analogous to that of **3-Cp*** (Figures S8−S12).

To confirm the presence of a ligand radical in **3-^{t}Bu** as well as to decide between options (1) and (2), X-ray diffraction analysis of single crystals obtained from a concentrated *n*-pentane solution at −35 °C was performed. Refinement of the data revealed the predicted *trans*-bis(imido) uranium complex (N4−U1−N5 = 155.5(3)°) bound by a tridentate pyridine(diimine) ligand with an η^5-Cp* (U−Ct = 2.567 Å) cap (Figure 4). Similar to **3-Cp***, the U−N_{imido} bonds of 1.941(8) and 1.944(8) Å are significantly shorter than those observed in pentavalent **2-Cp*** and (^{Mes}PDI^{Me})U(NMes)$_2$I(THF) (2.011(15) and 2.014(14) Å). These distances more closely resemble the uranium(VI) tris(imido) species, (^{Mes}PDI^{Me})U(NDIPP)$_3$ (DIPP = 2,6-diisopropylphenyl) (1.965(7), 1.967(7) Å).[17] The three U−N_{PDI} distances in **3-^{t}Bu** are consistent with dative interactions; however, the intraligand distances are distorted, suggesting reduction akin to **3-Cp***. The elongation of the pyridine bonds C3−C4 (1.466(14) Å) and C6−C7 (1.496(13) Å) in **3-^{t}Bu** and the contraction of the adjacent $C_{pyridine}$−C_{imine} bonds (C2−C3 = 1.427(14); 1.433(14) Å) support ligand reduction. Thus, the crystallographic data support that option (2), localization of a ligand radical at the *m*-pyridine position, is favored.

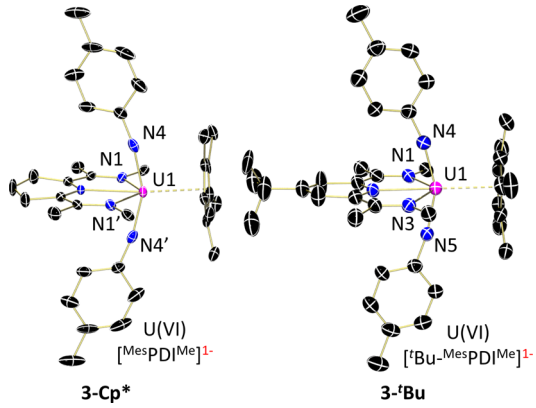

Figure 4. Molecular structures of **3-Cp*** (left) and **3-^{t}Bu** (right) displayed at 30% probability ellipsoids. Selected aryl substituents, cocrystallized molecules, and hydrogen atoms have been omitted for clarity.

As in the case of **3-Cp***, formation of **3-^{t}Bu** proceeds with four reducing equivalents derived cooperatively from the uranium and reduced ligand of **1-^{t}Bu**. Alteration of the electronics in the pyridine ring by addition of an electron-donating *tert*-butyl substituent neither disfavored reduction (option (3)) nor localized a ligand radical at the tertiary *para*-pyridine position (option (1)); the anionic charge observed in **3-Cp*** also persists in **3-^{t}Bu**.

As **2-Cp***, **2-Cp^P**, **3-Cp^P**, **3-Cp***, and **3-^{t}Bu** all contain one unpaired electron, their electronic ground state was probed by X-band electron paramagnetic resonance spectroscopy at room temperature (Figure S39). The uranium(V) complexes, **2-Cp***, **2-Cp^P**, and **3-Cp^P**, are EPR silent (toluene solution), while **3-Cp*** and **3-^{t}Bu** each display a weakly intense, broadened nearly isotropic signal centered at |*g*| = 1.974 in methylcyclohexane, similar to that observed for Cp*UO_2(^{Mes}PDI^{Me}). Uranium(V) complexes are generally known to be EPR silent above liquid nitrogen temperatures,[34] suggesting the observed room-temperature signals are predominantly ligand radical derived. Although poorly resolved, the observed splitting in **3-Cp*** and **3-^{t}Bu** is similar to that noted for the radical cation localized on the salophen ligand of the uranium(VI) uranyl derived from chemical oxidation of UO_2(salophen^{tBu})(H_2O) (salophen^{tBu} = *N*,*N*′-bis(3,5-di-*tert*-butylsalicylidene)-1,2-phenylenediamine).[35] As a further probe, all species were investigated as glasses at 6 K. All five complexes reveal analogous rhombic signals with g_x, g_y, and g_z tensor values near 3.6, 0.6−0.7, and 0.5−0.6, respectively (Figure S40). As each complex contains a single unpaired electron, these data are consistent with significant electron density residing at uranium at 6 K, contrary to the room-temperature observations. The rhombic spectra of complexes **2** and **3** are consistent with similar cationic and neutral uranium(V) species [(COT)U(NEt$_2$)$_2$(THF)]$^+$, [Cp*U(NMe$_2$)$_3$(THF)]$^+$, and (COT)U(NEt$_2$)$_3$ described by Gourier et al.[36]

DOI: 10.1021/jacs.6b06989
J. Am. Chem. Soc. 2016, 138, 13941−13951

Oxidation of Bis(imido) Complexes. To complete the series of electronic structures for uranium bis(imido) species, oxidation of **3-Cp*** and **3-^{t}Bu** was attempted. Removal of the ligand radical would further confirm the U(VI)/[^{Mes}PDI^{Me}]$^{1-}$ electronic structure and facilitate structural comparison with reduced ligand derivatives. Treating **3-Cp*** and **3-^{t}Bu** each with 1 equiv of $AgSbF_6$ (eq 1) resulted in deposition of silver onto

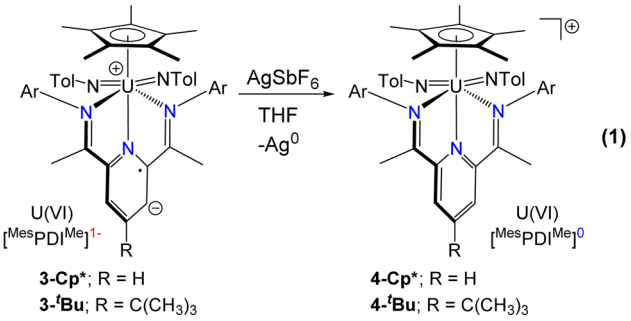

(1)

the walls of the scintillation vial over ca. 2 h, signifying successful oxidation. Infrared spectroscopy of the red-brown materials obtained confirmed the presence of an $[SbF_6]^{1-}$ anion in each complex (Figures S16 and S21) due to respective υ_3(Sb−F) absorbances at 662 and 658 cm^{-1} allowing for the assignments as [Cp*U(NTol)$_2$(^{Mes}PDI^{Me})][SbF_6] (**4-Cp***) and [Cp*U(NTol)$_2$(^{t}Bu-^{Mes}PDI^{Me})][SbF_6] (**4-^{t}Bu**). Repeating the oxidations in sealed NMR tubes (CD_2Cl_2, ambient temperature, Figures S41,42) revealed the anticipated products, **4-Cp*** and **4-^{t}Bu**, without any evidence of unexplained byproducts, including dihydrogen.

Analysis of **4-Cp*** and **4-^{t}Bu** by ^{1}H NMR spectroscopy revealed diamagnetic spectra with 10 resonances each consistent with C_{2v} symmetry (Figures S13 and S18). Sharply contrasting the C_s symmetry of complexes **3**, this change in symmetry is consistent with rearomatization of the pyridine ring and dismissal of the localized radical charge on the pyridine. A comparison of ^{1}H NMR data for **3-Cp*** (C_s, ligand radical) and **4-Cp*** (C_{2v}, neutral ligand) is displayed in Figure 2. Other than the change in symmetry, as compared to **3-Cp***, resonances attributed to the pyridine ring in **4-Cp*** appear shifted toward their diamagnetic free ligand reference values, thus confirming a third electronic structure for this family of *trans*-bis(imido) species.

Electronic absorption spectroscopy reflects the changes in the respective electronic structures from oxidation of **3-Cp*** and **3-^{t}Bu** to **4-Cp*** and **4-^{t}Bu** (Figure 3, bottom). Complexes **4** no longer display the three distinct transitions observed in their reduced counterparts; rather, relatively featureless spectra are obtained with each only containing a broadened, weak shoulder at ca. 580 nm (2300−2500 M^{-1} cm^{-1}). As expected for uranium(VI), 5f^0 species, neither display f−f transitions in the near-infrared region. The loss of visible transitions in **4** is directly associated with removal of radical character from the pyridine(diimine) chelates via oxidation.

For comparison to the reduced species, structural analyses of **4-Cp*** and **4-^{t}Bu** were performed. For ease of crystallization, the tetraphenylborate analogue of **4-^{t}Bu** was synthesized (preparation and spectroscopic data of the BPh_4 analogue are provided in the Supporting Information). Single, X-ray quality crystals were obtained from concentrated THF/diethyl ether (3:1) and concentrated THF/hexamethyldisiloxane (3:1) solutions at room temperature for **4-Cp*** and **4-^{t}Bu**, respectively (Figure 5, left and middle; Table 1). Each pseudo-octahedral uranium bis(imido) complex is capped by an η^5-Cp* ligand (U1−Ct: **4-Cp***, 2.565; **4-^{t}Bu**, 2.503 Å). The U−N_{imido} distances of **4-Cp*** (1.928(4), 1.926(4) Å) and **4-^{t}Bu** (1.955(4), 1.944(4) Å) are significantly longer than those found in the only other crystallographically characterized bis(imido) cations, [U(NMe)$_2$(I)(THF)$_4$][I_3] (1.830(4) and 1.841(5) Å)[37] and [U(NDIPP)$_2$Br(^{Me}bpy)$_2$][I_3] (^{Me}bpy = 4,4′-dimethyl-2,2′-bipyridyl) (1.856(8) Å).[38] This significant elongation in **4-Cp*** and **4-^{t}Bu** is attributed to disruption of the inverse *trans*-influence due to the deviation from linearity of the imido ligands (N4−U1−N5 = 155.45(16)° and 153.14(15)°, respectively) imparted by the bulky Cp* ligand.[39]

Parameters for the pyridine(diimine) ligands of **4-Cp*** and **4-^{t}Bu** are very similar, and, as such, only those of **4-Cp*** will be discussed in detail (ligand parameters of **4-^{t}Bu** shown in Table 1). **4-Cp*** possesses three long U−N bonds to the pyridine(diimine) chelate (2.549(4), 2.539(4), and 2.597(4) Å), consistent with a neutral ligand and similar to (^{Mes}PDI^{Me})U(NMes)$_3$ (2.553(4) and 2.580(5) Å). Intraligand bond lengths

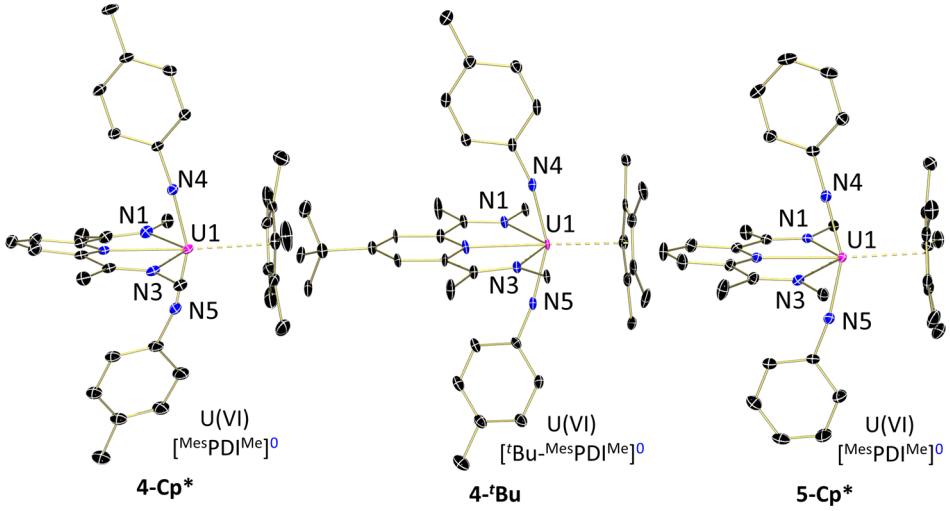

Figure 5. Molecular structures of **4-Cp*** (left), **4-^{t}Bu** (middle), and **5-Cp*** (right) displayed at 30% probability ellipsoids. Selected aryl substituents, cocrystallized molecules, and hydrogen atoms have been omitted for clarity.

DOI: 10.1021/jacs.6b06989
J. Am. Chem. Soc. 2016, 138, 13941−13951

that previously indicated ligand reduction in **3-Cp*** now resemble a neutral ligand following oxidation. The C_{imine}–$C_{pyridine}$ distances have been elongated to the order of a single bond (1.484(6) and 1.481(6) Å), while the $C_{pyridine}$–$C_{pyrdine}$ bonds, C3–C4 and C6–C7, have been contracted to 1.391(7) and 1.387(7) Å, respectively, indicative of aromaticity in the ring. For transition metal complexes of pyridine(diimine), this approach has previously been employed by Chirik and co-workers in evaluating metrical variations between cobalt complexes, $[([^{iPr}PDI^{Me}]^{\bullet-})Co^{I}N_2$ and $[([^{iPr}PDI^{Me}]^{0})Co^{I}N_2]^{+}$,[40] as well as in manganese bis(ligand) complexes described by Wieghardt and co-workers, $[Mn^{III}([^{OMe}PDI^{Me}]^{1-})_2][PF_6]$ and $[Mn^{II}([^{OMe}PDI^{Me}]^{0})_2](PF_6)_2$.[41]

Upon oxidation of complexes **3** to ion pair complexes **4**, the uranium–imido bond distances remain the same within error (Table 1) consistent with maintaining the uranium(VI) oxidation state. If oxidation occurred at uranium rather than $^{Mes}PDI^{Me}$, a contraction of the U–N_{imido} bond by ca. 0.1 Å would be anticipated, as in the case of uranium(V) $U(NDIPP)_2(Br)(^{R}bpy)_2$, whose U–N distances (1.981(5) and 1.968(6) Å) decrease upon oxidation to 1.858(8) Å in $[U(NDIPP)(Br)(^{R}bpy)][I_3]$ due to the difference in ionic radii.[38]

For comparative purposes, oxidation of the uranium(V) neutral ligand species, **2-Cp***, was attempted. Under conditions analogous to the oxidation of complexes **3**, oxidation of **2-Cp*** with $AgSbF_6$ resulted in isolation of $[Cp^*U(NPh)_2(^{Mes}PDI^{Me})][SbF_6]$ (**5-Cp***) (eq 2) as confirmed by

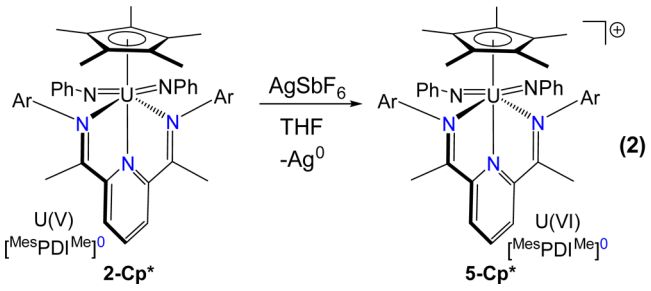

(2)

IR spectroscopy ($[SbF_6]^-$ = 657 cm^{-1}; Figure S27). Complete assignment of C_{2v} symmetric **5-Cp*** was achieved via 2D NMR spectroscopy (Figures S23–26). Facile oxidation of uranium(V) bis(imido) complexes with Ag(I) has previously been observed by Boncella and co-workers.[42]

Contrary to the observations for **3-Cp*** and **3-^{t}Bu**, chemical oxidation of **2-Cp*** occurs at uranium rather than the ligand. Thus, structural parameters of **5-Cp*** were sought to determine if any bonding changes would be apparent. Refinement of data obtained by analysis of single, X-ray quality crystals obtained by slow diffusion of *n*-pentane into a THF solution of **5-Cp*** at −35 °C revealed the uranium(VI) *trans*-bis(phenylimido) complex bound by an η^5-Cp* (2.531 Å) (Figure 5, Table 1). The *trans*(imido) substituents (N4–U1–N4 = 154.57(18)°) are more tightly coordinated (1.930(4), 1.943(4) Å) than those observed in the uranium(V) congener (2.036(5), 1.994 Å), consistent with oxidation from U(V) to U(VI). Throughout the entirety of the pyridine(diimine) ligand, negligible differences in the metrical parameters are observed, consistent with a maintained neutral chelate.

Investigation of **5-Cp*** by electronic absorption spectroscopy revealed no transitions in the near-infrared region, consistent with uranium oxidation from $5f^1$ to $5f^0$ (Figure 3, bottom). Transitions observed in the visible region are consistent with those in complexes **4**, with a notable shoulder at ca. 495 nm (6168 M^{-1} cm^{-1}), supporting U(VI) with a neutral $[^{Mes}PDI^{Me}]$.

As a further probe of the effective nuclear charge of the uranium centers in the bis(imido) family, X-ray absorption near edge spectroscopy (XANES) was obtained for **2-Cp^P**, **2-Cp***, **3-Cp***, **4-Cp***, as well as $Cp^*UO_2(^{Mes}PDI^{Me})$ for comparison. The background subtracted and normalized U $L_{3,2}$-edge XANES spectra for these compounds are presented in Figure 6 with the numerical data tabulated in Table 2. Spectra are

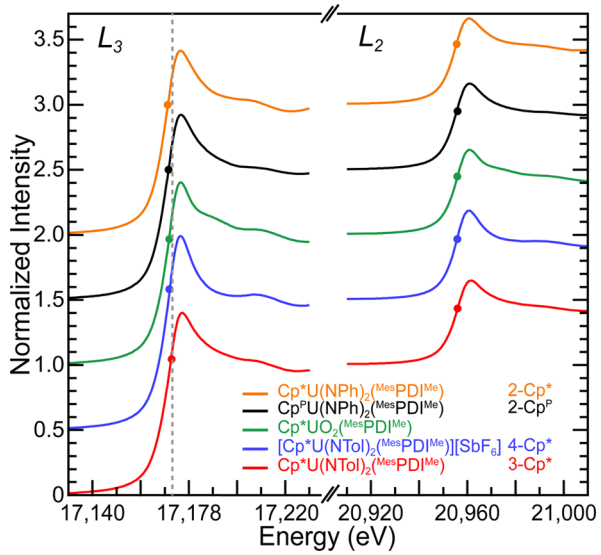

Figure 6. U L_{III}- and L_{II}-edge XANES from **2-Cp*** (orange), **2-Cp^P** (black), $Cp^*UO_2(^{Mes}PDI^{Me})$ (green), **4-Cp*** (blue), and **3-Cp*** (red) obtained at 77 K in transmission mode with an internal yttrium foil standard. The circular markers represent the inflection point.

defined by pronounced absorption edges and characterized by their inflection points. From the perspective of the free ion, the edge features in these spectra originate from electric-dipole allowed transitions from U 2p-orbitals to unoccupied states that contain U 5d character. These final states further split into two primary $L_{3,2}$-edges, due to spin–orbit coupling of the 2p core-hole. The following discussion will focus on the L_3-edge values because the trends are very similar in the L_2-edge region.

The uranium(V) complexes **2-Cp^P** and **2-Cp*** display the lowest energy inflection points at 17 171.6 and 17 171.2 eV, respectively. These are approximately 0.3–0.9 eV lower in energy than the uranium(VI) congeners, **3-Cp***, **4-Cp***, and $Cp^*UO_2(^{Mes}PDI^{Me})$, which show respective inflection point energies of 17 172.1, 17 171.9, and 17 171.9 eV. Variation of the phenyl(imido) ligand of **2-Cp*** to *p*-tolyl(imido) in **3-Cp*** results in a shift of 0.9 eV to higher energy of the L_3-edge due to the U(V)–U(VI) oxidation state change. This 0.9 eV change in the edge energy is smaller than that observed by Meyer and co-workers in the oxidation of pentavalent $[((^{Ad}ArO)_3tacn)U{=}O]$ to its hexavalent congener (Δ = 2.0 eV).[43] It is tempting to interpret the small 0.9 eV shift as indicative of a dramatic covalency in the **2-Cp*** and **3-Cp*** compounds. Consistently, calculations from our previous work show appreciable delocalization of charge in the uranium–ligand interactions.[18,44] However, without further experimentation, it is difficult to determine if changes in orbital mixing are the sole contributors to the differences in inflection point. Also of note

DOI: 10.1021/jacs.6b06989
J. Am. Chem. Soc. 2016, 138, 13941–13951

Table 2. Energy of the U L_3- and L_2-Edge Inflection Point and Peak Position of 2-Cp^P, 2-Cp*, 3-Cp*, 4-Cp*, and Cp*UO_2(^{Mes}PDI^{Me})[a]

complex	inflection point U L_3-edge (eV)	peak position at U L_3-edge (eV)	inflection point U L_2-edge (eV)	peak position at U L_2-edge (eV)	uranium//[^{Mes}PDI^{Me}] oxidation state
2-Cp^P	17 171.6	17 176.9	20 955.9	20 961.2	U(V)//[^{Mes}PDI^{Me}]^0
2-Cp*	17 171.2	17 176.5	20 955.6	20 960.7	U(V)//[^{Mes}PDI^{Me}]^0
3-Cp*	17 172.1	17 177.2	20 955.9	20 961.5	U(VI)//[^{Mes}PDI^{Me}]$^{1-}$
4-Cp*	17 171.9	17 176.6	20 955.8	20 960.7	U(VI)//[^{Mes}PDI^{Me}]$^{1-}$
Cp*UO_2(^{Mes}PDI^{Me})	17 171.9	17 176.6	20 955.8	20 961.0	U(VI)//[^{Mes}PDI^{Me}]$^{1-}$

[a]All data are calibrated against the Y K-edge from an internal yttrium foil standard measured in situ (17 038.4 eV).

is the very minimal shift observed in the L_3-edge (Δ = 0.2 eV) between **3-Cp*** and **4-Cp***. This observation is consistent with a hexavalent uranium center in both compounds, supporting a ligand-based oxidation process. Likewise, the analogous bis(imido) and bis(oxo) complexes, **3-Cp*** and Cp*UO_2(^{Mes}PDI^{Me}), display similar energies (Δ = 0.2 eV) as well.

CONCLUSION

In summary, the electronic structures of a family of uranium *trans*-bis(imido) species have been interrogated through a combined spectroscopic and structural analysis. The reduction capabilities of analogous cyclopentadienyl uranium(IV) pyridine(diimine) species, which feature trianionic ligands, were assessed using both organoazides and diazenes. In the case of the less electron-donating Cp^P ring, bis(imido) species were only formed from azide activation, as these species were not reducing enough to cleave diazenes. The corresponding uranium(V) bis(imido) complexes have neutral pyridine(diimine) ligands, indicating that an overall four-electron transfer occurred in the azide activation, with cooperative ligand and metal oxidation. The more electron-rich Cp* derivatives are reducing enough to cleave diazenes, forming *trans*-bis(imido) species. These compounds have strikingly different electronic structures, specifically due to the presence of methyl groups on the imido substituents. For the phenyl-substituted **2-Cp***, the same electronic structure is noted as for the Cp^P derivative. However, the presence of electron-donating methyl groups in the *p*-tolyl derivative stabilizes a buildup of electron density on a *meta*-carbon of the pyridine ring, generating an overall U(VI) species with a ligand radical.

From these studies, it is clear that subtle variations in the electron donicity in either the cyclopentadienyl or imido ligand substituents produce drastic changes in the location of unpaired electrons in this family. It is important to know that in cases where the reduced pyridine(diimine) ligand is observed, the radical is localized on a specific carbon atom. This is in sharp contrast to what is observed in transition metal chemistry, where reduction in pyridine(diimine) ligands is often delocalized throughout the entire plane of the pyridine and imine substituents. The electron localization is substantiated both structurally and spectroscopically. Furthermore, the U(V) and U(VI) oxidation state assignments are corroborated by X-ray absorption spectroscopic studies. From these studies, we have established three different electronic structures for the uranium(VI) bis(imido) family. Future work will focus on understanding the role electronic structure plays in reactivity of the uranium−nitrogen multiple bonds.

ASSOCIATED CONTENT

Supporting Information

The Supporting Information is available free of charge on the ACS Publications website at DOI: 10.1021/jacs.6b06989.

Synthetic procedures, spectroscopic data, and crystallographic details (PDF)

AUTHOR INFORMATION

Corresponding Author

*sbart@purdue.edu

Notes

The authors declare no competing financial interest.

ACKNOWLEDGMENTS

We acknowledge support from the Division of Chemical Sciences, Geosciences, and Biosciences, Office of Basic Energy Sciences, Heavy Elements Chemistry Program of the U.S. Department of Energy through Grant DE-SC0008479 (SCB). M.Z. thanks NSF Grant DMR 1337296 for X-ray diffractometer funding (used to collect molecular structures for **4-Cp*** and **5-Cp***). The XANES work was supported by the Heavy Element Chemistry Program by the Division of Chemical Sciences, Geosciences, and Biosciences, Office of Basic Energy Sciences, U.S. Department of Energy and the U.S. Department of Energy (Kozimor). Portions of this work were supported by postdoctoral and graduate Fellowships from the Glenn T. Seaborg Institute (M.G.F., B.W.S.), and the Director's Postdoctoral Fellowship (H.S.L.P.). Los Alamos National Laboratory is operated by Los Alamos National Security, LLC, for the National Nuclear Security Administration of U.S. Department of Energy (contract DE-AC52-06NA25396). Use of the Stanford Synchrotron Radiation Lightsource, SLAC National Accelerator Laboratory, was supported by the U.S. Department of Energy, Office of Science, Office of Basic Energy Sciences under Contract no. DE-AC02-76SF00515. The SSRL Structural Molecular Biology Program is supported by the DOE Office of Biological and Environmental Research, and by the National Institutes of Health, National Institute of General Medical Sciences (including P41GM103393).

REFERENCES

(1) Chirik, P. J. *Inorg. Chem.* **2011**, *50*, 9737−9740.
(2) Olivos, S. A. I.; Lyaskovskyy, V.; Reek, J. N. H.; van der Vlugt, J. L.; de, B. B. *Angew. Chem., Int. Ed.* **2013**, *52*, 12510−12529.
(3) Schaefer, B. A.; Margulieux, G. W.; Tiedemann, M. A.; Small, B. L.; Chirik, P. J. *Organometallics* **2015**, *34*, 5615−5623.
(4) Hoyt, J. M.; Schmidt, V. A.; Tondreau, A. M.; Chirik, P. J. *Science* **2015**, *349*, 960−963.
(5) Anderson, W. C.; Rhinehart, J. L.; Tennyson, A. G.; Long, B. K. *J. Am. Chem. Soc.* **2016**, *138*, 774−777.

DOI: 10.1021/jacs.6b06989
J. Am. Chem. Soc. 2016, 138, 13941−13951

(6) Evans, W. J.; Kozimor, S. A.; Ziller, J. W. *Chem. Commun.* **2005**, 4681−4683.
(7) Bart, S. C.; Chlopek, K.; Bill, E.; Bouwkamp, M. W.; Lobkovsky, E.; Neese, F.; Wieghardt, K.; Chirik, P. J. *J. Am. Chem. Soc.* **2006**, *128*, 13901−13912.
(8) Ranis, L. G.; Werellapatha, K.; Pietrini, N. J.; Bunker, B. A.; Brown, S. N. *Inorg. Chem.* **2014**, *53*, 10203−10216.
(9) Morsing, T. J.; MacMillan, S. N.; Uebler, J. W. H.; Brock-Nannestad, T.; Bendix, J.; Lancaster, K. M. *Inorg. Chem.* **2015**, *54*, 3660−3669.
(10) Schelter, E. J.; Wu, R.; Scott, B. L.; Thompson, J. D.; Cantat, T.; John, K. D.; Batista, E. R.; Morris, D. E.; Kiplinger, J. L. *Inorg. Chem.* **2010**, *49*, 924−933.
(11) Bendix, J.; Clark, K. M. *Angew. Chem., Int. Ed.* **2016**, *55*, 2748−2752.
(12) Small, B. L.; Brookhart, M.; Bennett, A. M. A. *J. Am. Chem. Soc.* **1998**, *120*, 4049−4050.
(13) Britovsek, G. J. P.; Bruce, M.; Gibson, V. C.; Kimberley, B. S.; Maddox, P. J.; Mastroianni, S.; McTavish, S. J.; Redshaw, C.; Solan, G. A.; Stroemberg, S.; White, A. J. P.; Williams, D. J. *J. Am. Chem. Soc.* **1999**, *121*, 8728−8740.
(14) Thompson, E. J.; Myers, T. W.; Berben, L. A. *Angew. Chem., Int. Ed.* **2014**, *53*, 14132−14134.
(15) Myers, T. W.; Berben, L. A. *Chem. Sci.* **2014**, *5*, 2771−2777.
(16) Knijnenburg, Q.; Gambarotta, S.; Budzelaar, P. H. M. *Dalton Trans.* **2006**, 5442−5448.
(17) Anderson, N. H.; Odoh, S. O.; Yao, Y.; Williams, U. J.; Schaefer, B. A.; Kiernicki, J. J.; Lewis, A. J.; Goshert, M. D.; Fanwick, P. E.; Schelter, E. J.; Walensky, J. R.; Gagliardi, L.; Bart, S. C. *Nat. Chem.* **2014**, *6*, 919−926.
(18) Anderson, N. H.; Odoh, S. O.; Williams, U. J.; Lewis, A. J.; Wagner, G. L.; Lezama Pacheco, J.; Kozimor, S. A.; Gagliardi, L.; Schelter, E. J.; Bart, S. C. *J. Am. Chem. Soc.* **2015**, *137*, 4690−4700.
(19) Cladis, D. P.; Kiernicki, J. J.; Fanwick, P. E.; Bart, S. C. *Chem. Commun.* **2013**, *49*, 4169−4171.
(20) Kiernicki, J. J.; Newell, B. S.; Matson, E. M.; Anderson, N. H.; Fanwick, P. E.; Shores, M. P.; Bart, S. C. *Inorg. Chem.* **2014**, *53*, 3730−3741.
(21) Pangborn, A. B.; Giardello, M. A.; Grubbs, R. H.; Rosen, R. K.; Timmers, F. J. *Organometallics* **1996**, *15*, 1518−1520.
(22) Barral, K.; Moorhouse, A. D.; Moses, J. E. *Org. Lett.* **2007**, *9*, 1809−1811.
(23) Lu, W.; Xi, C. *Tetrahedron Lett.* **2008**, *49*, 4011−4015.
(24) Kiernicki, J. J.; Cladis, D. P.; Fanwick, P. E.; Zeller, M.; Bart, S. C. *J. Am. Chem. Soc.* **2015**, *137*, 11115−11125.
(25) Jordan, R. F.; Echols, S. F. *Inorg. Chem.* **1987**, *26*, 383−386.
(26) Sheldrick, G. M. *Acta Crystallogr., Sect. A: Found. Crystallogr.* **2008**, *A64*, 112−122.
(27) Huebschle, C. B.; Sheldrick, G. M.; Dittrich, B. *J. Appl. Crystallogr.* **2011**, *44*, 1281−1284.
(28) Sheldrick, G. M. *Acta Crystallogr., Sect. C: Struct. Chem.* **2015**, *71*, 3−8.
(29) Kiernicki, J. J.; Fanwick, P. E.; Bart, S. C. *Chem. Commun.* **2014**, *50*, 8189−8192.
(30) Graves, C. R.; Vaughn, A. E.; Schelter, E. J.; Scott, B. L.; Thompson, J. D.; Morris, D. E.; Kiplinger, J. L. *Inorg. Chem.* **2008**, *47*, 11879−11891.
(31) Lewis, A. J.; Mullane, K. C.; Nakamaru-Ogiso, E.; Carroll, P. J.; Schelter, E. J. *Inorg. Chem.* **2014**, *53*, 6944−6953.
(32) Spencer, L. P.; Gdula, R. L.; Hayton, T. W.; Scott, B. L.; Boncella, J. M. *Chem. Commun.* **2008**, 4986−4988.
(33) Dugan, T. R.; Bill, E.; MacLeod, K. C.; Christian, G. J.; Cowley, R. E.; Brennessel, W. W.; Ye, S.; Neese, F.; Holland, P. L. *J. Am. Chem. Soc.* **2012**, *134*, 20352−20364.
(34) Meyer, K.; Mindiola, D. J.; Baker, T. A.; Davis, W. M.; Cummins, C. C. *Angew. Chem., Int. Ed.* **2000**, *39*, 3063−3066.
(35) Herasymchuk, K.; Chiang, L.; Hayes, C. E.; Brown, M. L.; Ovens, J.; Patrick, B. O.; Leznoff, D. B.; Storr, T. *Dalton Trans.* **2016**, *45*, 12576−12586.
(36) Gourier, D.; Caurant, D.; Berthet, J. C.; Boisson, C.; Ephritikhine, M. *Inorg. Chem.* **1997**, *36*, 5931−5936.
(37) Spencer, L. P.; Yang, P.; Minasian, S. G.; Jilek, R. E.; Batista, E. R.; Boland, K. S.; Boncella, J. M.; Conradson, S. D.; Clark, D. L.; Hayton, T. W.; Kozimor, S. A.; Martin, R. L.; MacInnes, M. M.; Olson, A. C.; Scott, B. L.; Shuh, D. K.; Wilkerson, M. P. *J. Am. Chem. Soc.* **2013**, *135*, 2279−2290.
(38) Jilek, R. E.; Spencer, L. P.; Lewis, R. A.; Scott, B. L.; Hayton, T. W.; Boncella, J. M. *J. Am. Chem. Soc.* **2012**, *134*, 9876−9878.
(39) Hayton, T. W.; Boncella, J. M.; Scott, B. L.; Palmer, P. D.; Batista, E. R.; Hay, P. J. *Science* **2005**, *310*, 1941−1943.
(40) Bowman, A. C.; Milsmann, C.; Atienza, C. C. H.; Lobkovsky, E.; Wieghardt, K.; Chirik, P. J. *J. Am. Chem. Soc.* **2010**, *132*, 1676−1684.
(41) De Bruin, B.; Bill, E.; Bothe, E.; Weyhermüller, T.; Wieghardt, K. *Inorg. Chem.* **2000**, *39*, 2936−2947.
(42) Spencer, L. P.; Yang, P.; Scott, B. L.; Batista, E. R.; Boncella, J. M. *Inorg. Chem.* **2009**, *48*, 11615−11623.
(43) Kosog, B.; La Pierre, H. S.; Denecke, M. A.; Heinemann, F. W.; Meyer, K. *Inorg. Chem.* **2012**, *51*, 7940−7944.
(44) Li Manni, G.; Walensky, J. R.; Kraft, S. J.; Forrest, W. P.; Perez, L. M.; Hall, M. B.; Gagliardi, L.; Bart, S. C. *Inorg. Chem.* **2012**, *51*, 2058−2064.

DOI: 10.1021/jacs.6b06989
J. Am. Chem. Soc. 2016, 138, 13941−13951